



Crystal growth, structural and electrical properties of $(\text{Cu}_{1-x}\text{Ag}_x)_7\text{GeS}_5\text{I}$ superionic solid solutions

I.P. Studenyak^{a,*}, A.I. Pogodin^a, O.P. Kokhan^a, V. Kavaliukė^b, T. Šalkus^b, A. Kežionis^b, A.F. Orliukas^b

^a Uzhhorod National University, 46 Pidhirna St., 88000 Uzhhorod, Ukraine

^b Vilnius University, Saulėtekio al. 9, LT-10222 Vilnius, Lithuania



ARTICLE INFO

Keywords:

Superionic conductor
XRD studies
Impedance spectroscopy
Electrical conductivity
Arrhenius law

ABSTRACT

Single crystals of $(\text{Cu}_{1-x}\text{Ag}_x)_7\text{GeS}_5\text{I}$ solid solutions were grown by vertical zone crystallization method. XRD studies have shown that they crystallize in face-centered cubic lattice of the argyrodite structure (space group $F\bar{4}3m$, $Z = 4$). Structural studies were performed on the basis of original structure model by means of Rietveld refinement method. Electrical measurements were carried out in the temperature interval 300–360 K and in the range of frequencies 10 Hz–10 GHz. Temperature and frequency dependences of electrical conductivity were analyzed. Influence of cation substitution on the electrical conductivity as well as relationship between structural and electrical properties of $(\text{Cu}_{1-x}\text{Ag}_x)_7\text{GeS}_5\text{I}$ solid solutions were studied.

1. Introduction

$\text{Cu}_7\text{GeS}_5\text{I}$ and $\text{Ag}_7\text{GeS}_5\text{I}$ crystals belong to the family of compounds with argyrodite structure. Some members of argyrodite family are known as superionic conductors [1]. Due to the high electrical conductivity, they are promising materials for wide applications as solid electrolytes, supercapacitors, ion-selective membranes, and others electrochemical devices. Today, the argyrodite structures (e.g. lithium containing superionic conductors [2]) can be used as candidates for preparing all-solid-state batteries. Moreover, they are also interesting materials for fundamental studies of the ionic transport mechanism and order-disorder processes.

At room temperature $\text{Cu}_7\text{GeS}_5\text{I}$ and $\text{Ag}_7\text{GeS}_5\text{I}$ compounds crystallize in face-centered cubic lattice of the argyrodite structure (space group $F\bar{4}3m$, $Z = 4$) [1,3,4]. The electrical conductivity of $\text{Cu}_7\text{GeS}_5\text{I}$ crystal grown by chemical transport reaction method was reported to reach the value of $6.98 \cdot 10^{-1} \text{ S/m}$ at $T = 300 \text{ K}$ ($f = 100 \text{ Hz}$) [5]. Optical studies of $\text{Cu}_7\text{GeS}_5\text{I}$ have shown that the absorption edge exhibits an Urbach shape; the optical pseudogap and the Urbach energy were determined by the effect of both temperature-dependent (thermal vibrations of lattice and dynamic structural disordering in the cation sublattice) and static structural disordering. $\text{Ag}_7\text{GeS}_5\text{I}$ is known as a pure ionic conductor with the electric conductivity of 2.77 S/m at $T = 300 \text{ K}$ [6].

The studies of the influence of cationic substitution on the physical properties of solid solutions based on $\text{Cu}_7\text{GeS}_5\text{I}$ and $\text{Ag}_7\text{GeS}_5\text{I}$ crystals

are interesting both in fundamental and applied aspects. Crystal growth technology, some physical and chemical parameters of $\text{Cu}_7\text{GeS}_5\text{I}$ -based solid solutions were presented in Refs. [7, 8]. Electrical, electrochemical and optical properties of the above mentioned solid solutions were studied [9–12]. The compositional studies of electrical conductivity in $\text{Cu}_7\text{Ge}(\text{S}_{1-x}\text{Se}_x)_5\text{I}$ and $\text{Cu}_7(\text{Ge}_{1-x}\text{Si}_x)\text{S}_5\text{I}$ solid solutions have shown that $\text{S} \rightarrow \text{Se}$ anionic substitution and $\text{Si} \rightarrow \text{Ge}$ cationic substitution both result in a nonlinear increase of the electric conductivity by more than an order of magnitude [11,12]. The nonlinear decrease of the optical pseudogap in the $\text{Cu}_7\text{Ge}(\text{S}_{1-x}\text{Se}_x)_5\text{I}$ and $\text{Cu}_7(\text{Ge}_{1-x}\text{Si}_x)\text{S}_5\text{I}$ solid solutions at $\text{S} \rightarrow \text{Se}$ anionic substitution and $\text{Si} \rightarrow \text{Ge}$ cationic substitution was observed, the compositional dependence of the Urbach energy revealed a typical behaviour for solid solution crystals. It was shown that the character of the compositional behaviour of the absorption edge parameters is determined by the nonlinear compositional behaviour of the contribution of compositional disordering to the Urbach energy of the solid solutions [11,12].

The aim of this paper is to develop the growth technology as well as to investigate structural and electrical properties of $(\text{Cu}_{1-x}\text{Ag}_x)_7\text{GeS}_5\text{I}$ solid solutions.

2. Experimental

The specific route of modified $(\text{Cu}_{1-x}\text{Ag}_x)_7\text{GeS}_5\text{I}$ crystals growth technique, as in the case of $\text{Cu}_7\text{GeS}_5\text{I}$ and $\text{Ag}_7\text{GeS}_5\text{I}$ compounds, allows

* Corresponding author.

E-mail address: studenyak@dr.com (I.P. Studenyak).

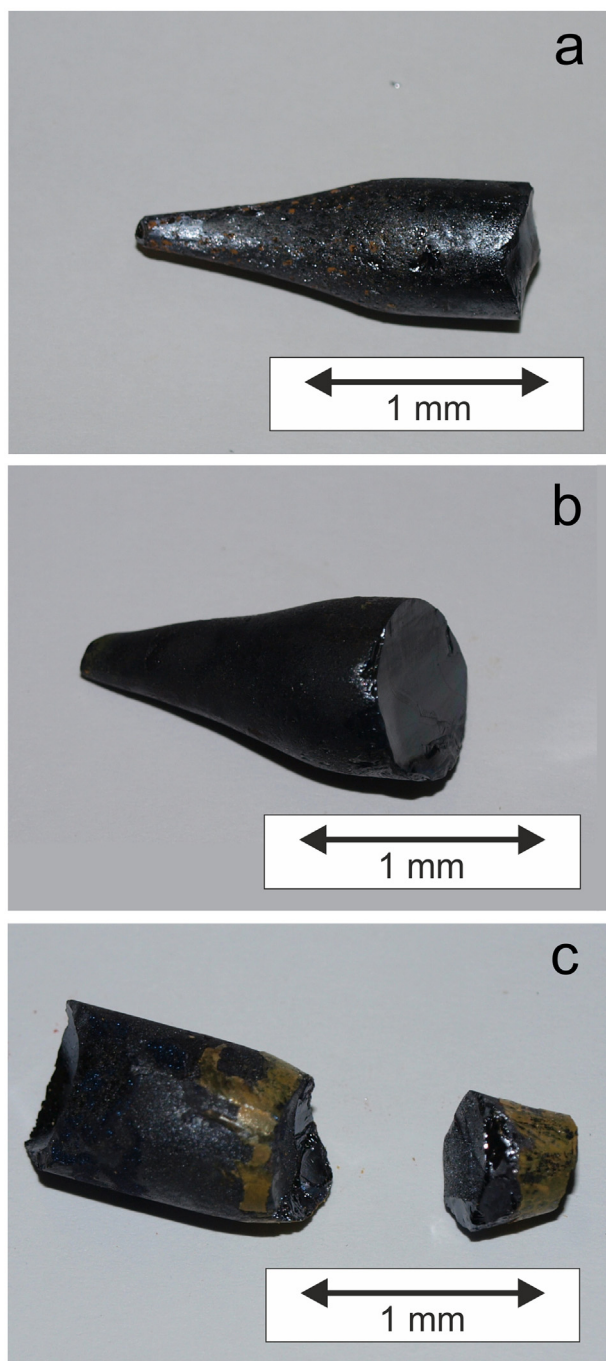


Fig. 1. Images of $(\text{Cu}_{1-x}\text{Ag}_x)_7\text{GeS}_5\text{I}$ solid solution single crystals: $(\text{Cu}_{0.75}\text{Ag}_{0.25})_7\text{GeS}_5\text{I}$ (a), $(\text{Cu}_{0.5}\text{Ag}_{0.5})_7\text{GeS}_5\text{I}$ (b), and $(\text{Cu}_{0.25}\text{Ag}_{0.75})_7\text{GeS}_5\text{I}$ (c).

us to obtain single crystals of solid solutions with desired composition without deviations from the stoichiometry in the whole concentration range. Initially, elemental Ag, Cu, Ge, and S as well as presynthesized AgI (CuI), additionally purified by directional solidification from the melt, were loaded into the ampoule. The regime of the crystal growth by directional solidification from the melt for $(\text{Cu}_{1-x}\text{Ag}_x)_7\text{GeS}_5\text{I}$ solid solutions consisted of several stages. At the first stage $(\text{Cu}_{1-x}\text{Ag}_x)_7\text{GeS}_5\text{I}$ synthesis was performed. The temperature of both zones was increased to 673 K within 6 h. At about 720 K the sulfur vapor pressure is 0.1 MPa, and the rapid temperature increase can cause depressurization of the ampoule. Therefore, the ampoule was kept at this temperature for 24 h, during this time sulfur is completely fixed. Then the temperature was increased during 24 h to the maximum temperature values of 1323 K for

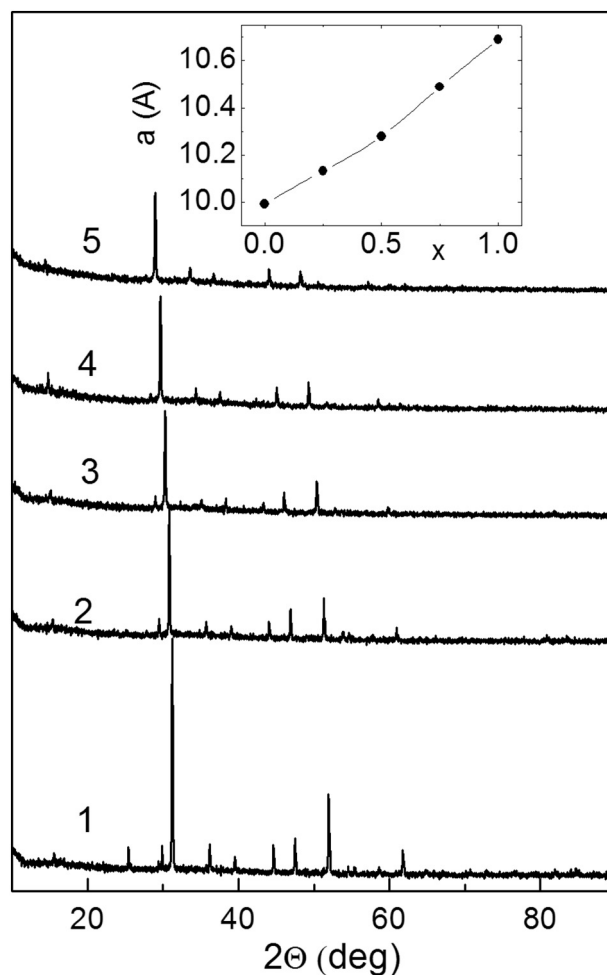


Fig. 2. X-ray diffraction patterns for $(\text{Cu}_{1-x}\text{Ag}_x)_7\text{GeS}_5\text{I}$ solid solutions: $\text{Cu}_7\text{GeS}_5\text{I}$ (1), $(\text{Cu}_{0.75}\text{Ag}_{0.25})_7\text{GeS}_5\text{I}$ (2), $(\text{Cu}_{0.5}\text{Ag}_{0.5})_7\text{GeS}_5\text{I}$ (3), $(\text{Cu}_{0.25}\text{Ag}_{0.75})_7\text{GeS}_5\text{I}$ (4) and $\text{Ag}_7\text{GeS}_5\text{I}$ (5). The inset shows the compositional dependence of the lattice parameter in $(\text{Cu}_{1-x}\text{Ag}_x)_7\text{GeS}_5\text{I}$ solid solutions.

the “hot” upper zone and 973 K for the “cold” bottom zone. Upon reaching the desired temperature in the upper zone, the solid solution is melted, and at higher temperatures the melt homogenization occurs. The temperature in the melt zone was maintained by 50 K above the melting point to prevent partial thermal dissociation of the compounds. The ampoule was kept at this temperature for 24 h to provide full homogenization of the melt.

A single-crystal “seed” for the $(\text{Cu}_{1-x}\text{Ag}_x)_7\text{GeS}_5\text{I}$ growth was formed in the bottom of a cone-shaped growth container (48 h). In order to obtain homogeneous solid solution single crystals, the vertical zone crystallization method was used. After moving the ampoule with the crystal to the annealing zone, it was annealed for 3 days to relax thermal stresses in the crystals. Single crystals of $(\text{Cu}_{1-x}\text{Ag}_x)_7\text{GeS}_5\text{I}$ ($x = 0.25, 0.5, \text{ and } 0.75$) solid solutions with the length of 30–40 mm and the diameter of 10–15 mm were obtained (Fig. 1).

Structural studies were carried out by powder X-ray diffraction method using a DRON 4-07 diffractometer (conventional θ - 2θ scanning mode, Bragg angle $2\theta \cong 10$ – 60° , Ni-filtered $\text{Cu K}\alpha$ radiation). Refinement of $\text{Cu}^+ \leftrightarrow \text{Ag}^+$ substitution mechanism and lattice atomic coordinates were carried out on the basis of the refined models of original structures by means of Rietveld method [13,14]. The model calculation and refinement were carried out using EXPO 2014 software package [15,16], visualization was performed using VESTA 3.4.4 software [17].

Measurements of complex impedance of $(\text{Cu}_{1-x}\text{Ag}_x)_7\text{GeS}_5\text{I}$ single

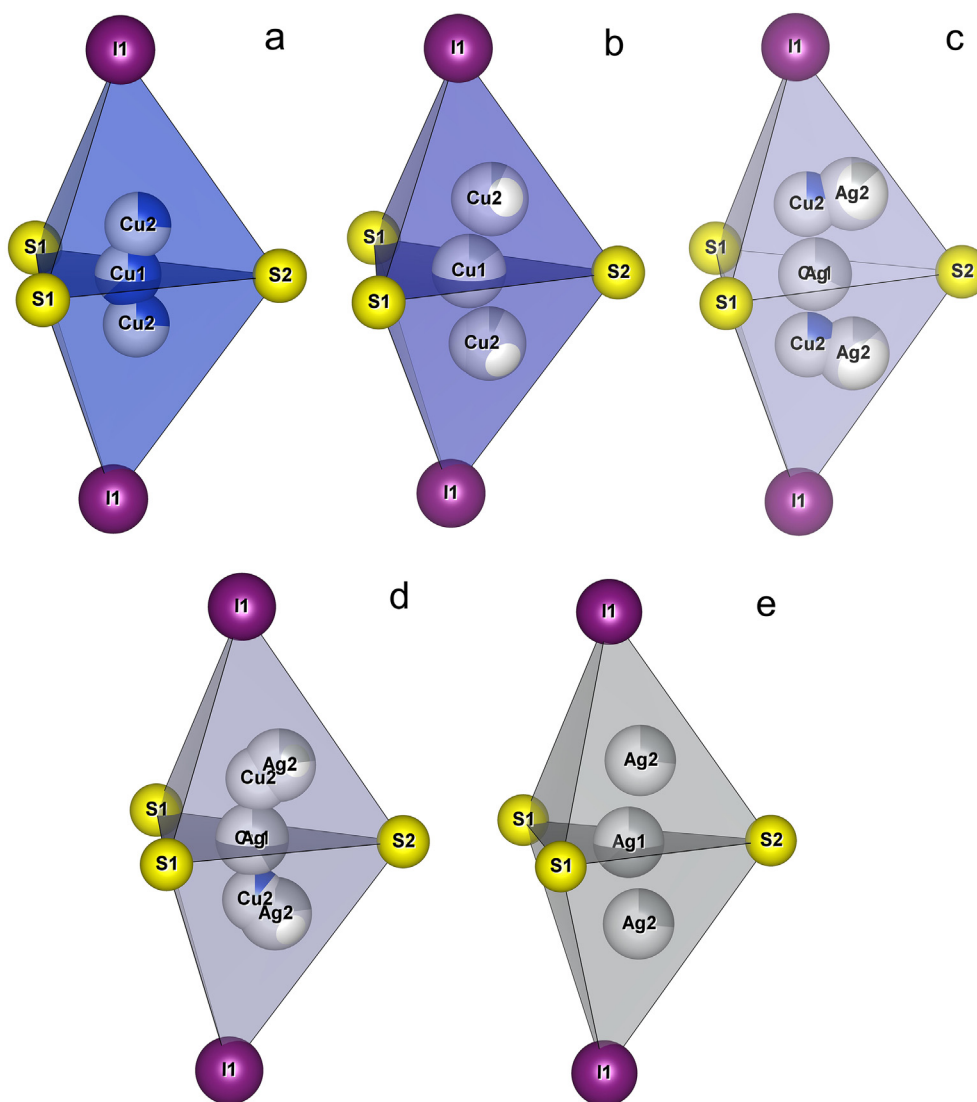


Fig. 3. $\text{Cu}^+ \leftrightarrow \text{Ag}^+$ substitution dynamics during the formation of a solid solution in $\text{Cu}_7\text{GeS}_5\text{I} - \text{Ag}_7\text{GeS}_5\text{I}$ system (as exemplified by $[\text{S}_3\text{I}_2]$ doubled tetrahedron).

crystals were carried out in the frequency range from 10 Hz to 10 GHz in the temperature interval 300–360 K using a coaxial impedance spectrometer [18,19].

3. Results and discussion

X-ray diffraction patterns of $(\text{Cu}_{1-x}\text{Ag}_x)_7\text{GeS}_5\text{I}$ solid solutions were indexed as face-centered cubic cell with space group $F\bar{4}3m$, the number of formula units per unit cell $Z = 4$ (Fig. 2). Due to the isostructurality of compounds and close values of ion radii (0.98 Å for Cu^+ and 1.13 Å for Ag^+), a continuous set of solid solutions with $\text{Cu}^+ \leftrightarrow \text{Ag}^+$ substitution is formed in the $\text{Cu}_7\text{GeS}_5\text{I} - \text{Ag}_7\text{GeS}_5\text{I}$ system. The compositional dependence of the cubic lattice parameter (Fig. 2) shows that the increase of Ag content in the $(\text{Cu}_{1-x}\text{Ag}_x)_7\text{GeS}_5\text{I}$ solid solutions leads to the lattice parameter increase.

In order to explain the structural changes at $\text{Cu}^+ \leftrightarrow \text{Ag}^+$ substitution, we will consider $[\text{Cu}(\text{Ag})\text{S}_3\text{I}_2]$ doubled tetrahedra. The structure of $\text{Cu}_7\text{GeS}_5\text{I}$ contains two symmetrically independent copper ions in Cu_1 (24 g) and Cu_2 (48 h) positions. The Cu_1 ion is located in a trigonal coordination of sulfur atoms (S1S2S1), while Cu_2 ion is tetragonally coordinated (S1S2S1I) and shifted toward the S1S2S1 triangle plane (Fig. 3a). When a solid solution is formed, the substitution occurs both in Cu_1 (24 g) and Cu_2 (48 h) positions accompanied by the position shift.

The position of Cu_1Ag_1 is located in the S1S2S1 triangle plane, the Cu_2Ag_2 substitution position is tetragonally coordinated (S1S2S1I) and is strongly shifted to the IS2 edge and to the S1IS2 triangle planes (Fig. 3b). Further introduction of Ag^+ in $(\text{Cu}_7\text{GeS}_5\text{I})_{0.5}(\text{Ag}_7\text{GeS}_5\text{I})_{0.5}$ solid solution causes significant disordering of cation sublattice. Cu_1Ag_1 position, similarly to the previous case, is located in the S1S2S1 triangle plane, whereas Cu_2Ag_2 substitution position is strongly elongated, Cu_2 ion deflects to the tetragonal coordination, whereas Ag_2 is shifted toward the IS2 edge (Fig. 3c). For $(\text{Cu}_7\text{GeS}_5\text{I})_{0.25}(\text{Ag}_7\text{GeS}_5\text{I})_{0.75}$ solid solution the insignificant ordering of cation sublattice is observed, the elongation of the shifted Cu_2Ag_2 substitution position decreases, but it still remains shifted to the IS2 edge and S1IS2 triangle planes (Fig. 3d). $\text{Ag}_7\text{GeS}_5\text{I}$ compound, similarly to $\text{Cu}_7\text{GeS}_5\text{I}$, contains two symmetrically independent silver ions in Ag_1 (24 g) and Ag_2 (48 h) positions, wherein Ag_1 ion is located in the trigonal coordination of sulfur atoms (S1S2S1) and Ag_2 ion is tetragonally coordinated (S1S2S1I) with the shift toward the S1S2S1 triangle plane and the IS2 edge (Fig. 3e).

The frequency dependences of the real part of complex electric conductivity σ' for $(\text{Cu}_{1-x}\text{Ag}_x)_7\text{GeS}_5\text{I}$ solid solutions are presented in Fig. 4a. It can be seen that the conductivity value increases with frequency. One dispersion region caused by the ion transport in the bulk of $(\text{Cu}_{1-x}\text{Ag}_x)_7\text{GeS}_5\text{I}$ solid solutions is observed in the frequency range under investigation. Such type of the frequency dependence of the

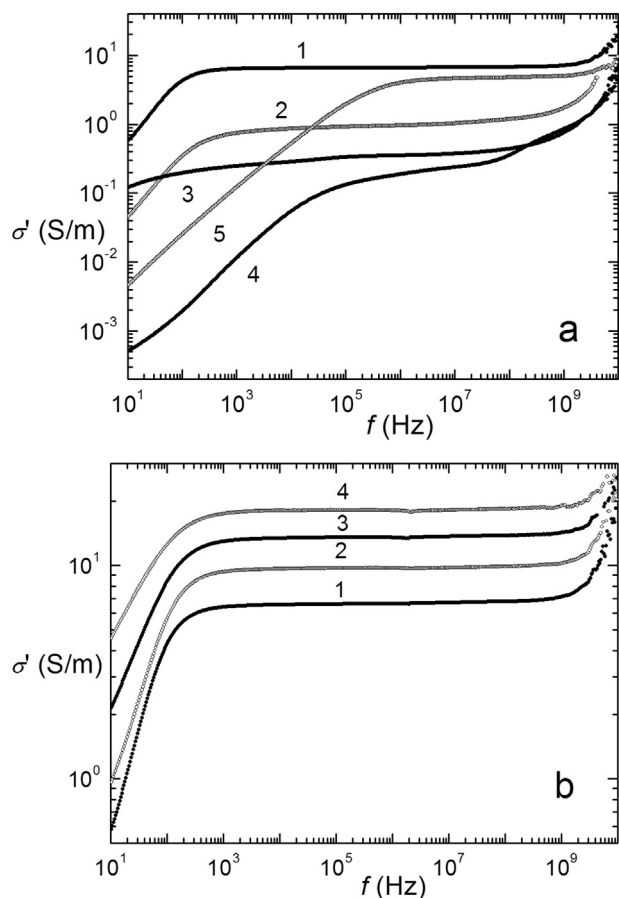


Fig. 4. a) Frequency dependences of the real part of complex electric conductivity σ' at 300 K for $(\text{Cu}_{1-x}\text{Ag}_x)_7\text{GeS}_5\text{I}$ solid solutions: $\text{Cu}_7\text{GeS}_5\text{I}$ (1), $(\text{Cu}_{0.75}\text{Ag}_{0.25})_7\text{GeS}_5\text{I}$ (2), $(\text{Cu}_{0.5}\text{Ag}_{0.5})_7\text{GeS}_5\text{I}$ (3), $(\text{Cu}_{0.25}\text{Ag}_{0.75})_7\text{GeS}_5\text{I}$ (4) and $\text{Ag}_7\text{GeS}_5\text{I}$ (5); b) frequency dependences of the real part of complex electric conductivity σ' of $\text{Cu}_7\text{GeS}_5\text{I}$ crystal at different temperatures: 300 K (1), 320 K (2), 340 K (3), and 360 K (4).

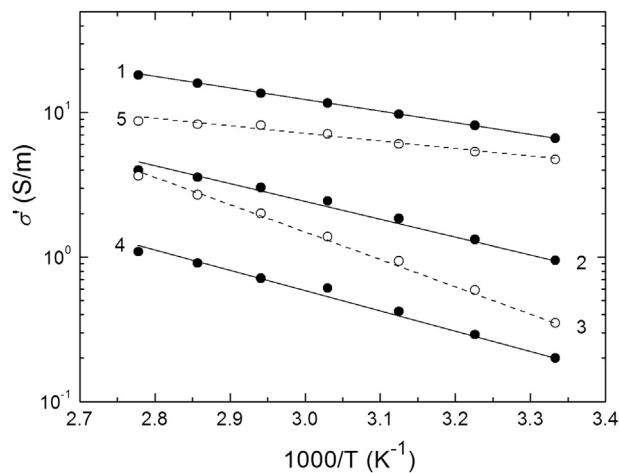


Fig. 5. Temperature dependences of the real part of complex electric conductivity σ' at 10^7 Hz for $(\text{Cu}_{1-x}\text{Ag}_x)_7\text{GeS}_5\text{I}$ solid solutions: $\text{Cu}_7\text{GeS}_5\text{I}$ (1), $(\text{Cu}_{0.75}\text{Ag}_{0.25})_7\text{GeS}_5\text{I}$ (2), $(\text{Cu}_{0.5}\text{Ag}_{0.5})_7\text{GeS}_5\text{I}$ (3), $(\text{Cu}_{0.25}\text{Ag}_{0.75})_7\text{GeS}_5\text{I}$ (4) and $\text{Ag}_7\text{GeS}_5\text{I}$ (5).

electric conductivity can be attributed to relaxation in the bulk. The dispersion in the lower-frequency parts of the spectra corresponds to processes at the interface between the superionic conductor and the electrodes. Fig. 4b shows the frequency dependences of the real part of

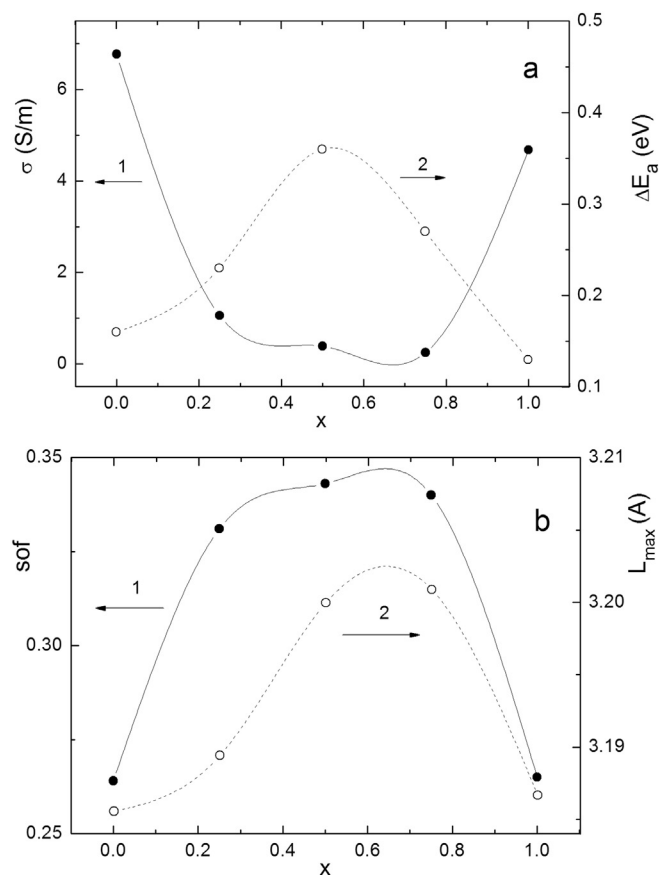


Fig. 6. a) Compositional dependences of the real part of complex electric conductivity σ' (1) at 10^7 Hz and activation energy (2) for $(\text{Cu}_{1-x}\text{Ag}_x)_7\text{GeS}_5\text{I}$ solid solutions; b) dependences of sof for mobile ions (1) and the maximal distance between the mobile ion positions Cu_2Ag_2 in the conductivity network (2) for $(\text{Cu}_{1-x}\text{Ag}_x)_7\text{GeS}_5\text{I}$ solid solutions.

complex electric conductivity σ' for $\text{Cu}_7\text{GeS}_5\text{I}$ crystal measured at different temperatures. The similar temperature behaviour of frequency dependences of electric conductivity is observed for all $(\text{Cu}_{1-x}\text{Ag}_x)_7\text{GeS}_5\text{I}$ solid solution sample. It is shown that in the temperature interval 300–360 K electric conductivity increases linearly with temperature according to the Arrhenius law (Fig. 5):

$$\sigma = \frac{\sigma_0}{T} \exp\left(-\frac{\Delta E_a}{kT}\right) \quad (1)$$

where ΔE_a is the activation energy of the electric conductivity, σ_0 is a constant, k is the Boltzmann constant, T is temperature. The linear character of the temperature dependences of the electric conductivity in Arrhenius coordinates indicates the thermal activation nature of the electric conductivity (Fig. 5).

Compositional studies have shown that with increasing silver content the electric conductivity of $(\text{Cu}_{1-x}\text{Ag}_x)_7\text{GeS}_5\text{I}$ solid solutions decreases and reaches minimum at $x = 0.75$ (Fig. 6a). The highest electrical conductivity value $\sigma = 6.8$ S/m at 300 K and 10^7 Hz was observed for $\text{Cu}_7\text{GeS}_5\text{I}$ crystal, while for $\text{Ag}_7\text{GeS}_5\text{I}$ $\sigma = 4.7$ S/m. For $(\text{Cu}_{1-x}\text{Ag}_x)_7\text{GeS}_5\text{I}$ solid solutions with $x = 0.5$ and 0.75 the electrical conductivity is more than by an order of magnitude higher compared to $\text{Cu}_7\text{GeS}_5\text{I}$ and $\text{Ag}_7\text{GeS}_5\text{I}$ crystals, and the minimal electrical conductivity value of 0.25 S/m is observed for $(\text{Cu}_{0.25}\text{Ag}_{0.75})_7\text{GeS}_5\text{I}$ solid solution. With the increase of the compositional parameter x the activation energy increases from 0.16 eV ($\text{Cu}_7\text{GeS}_5\text{I}$) and reaches the maximal value of 0.36 eV for $(\text{Cu}_{0.5}\text{Ag}_{0.5})_7\text{GeS}_5\text{I}$ solid solution, while with further increase of x ΔE_a decreases to 0.13 eV for $\text{Ag}_7\text{GeS}_5\text{I}$ crystal (Fig. 6a). A similar compositional behavior of the activation energy was

observed for other representatives of argyrodite family [11,12,20,21].

For $(\text{Cu}_{1-x}\text{Ag}_x)_7\text{GeS}_5\text{I}$ solid solutions the compositional behavior of the electric conductivity and the activation energy is in a good agreement with the results of structural studies. Based on the structural investigations, one can conclude on the mechanism of ionic transport in $\text{Cu}_7\text{GeS}_5\text{I}$ and $\text{Ag}_7\text{GeS}_5\text{I}$ compounds as well as in $(\text{Cu}_{1-x}\text{Ag}_x)_7\text{GeS}_5\text{I}$ solid solutions. Although Cu_1 (24 g) position is located in the S1S2S1 triangle plane of the $\text{Cu}_7\text{GeS}_5\text{I}$ compound, the mobile copper ion in this structure is located in the Cu_2 (48 h) position, which is shifted toward the above plane and the S2I edge. It is explained by the lower *sof* (site occupation factor) of Cu_2 (0.264) contrary to Cu_1 (0.632). When a solid solution is formed, the Cu_2Ag_2 substitution position is responsible for the high electric conductivity due to the shift toward the S1S2 triangle plane and the S2I edge. Similarly to $\text{Cu}_7\text{GeS}_5\text{I}$, in $\text{Ag}_7\text{GeS}_5\text{I}$ compound, the most mobile is the ion in Ag_2 (48 h) position. The dependences of *sof* for mobile ions and the maximum distance between the moving positions of Cu_2Ag_2 in the conduction network on the solid solution composition are presented in Fig. 6b.

The dependence of *sof* for mobile ions in $(\text{Cu}_{1-x}\text{Ag}_x)_7\text{GeS}_5\text{I}$ solid solutions versus x has shown that when the solid solution is formed, the mobility of ions in the substitution position Cu_2Ag_2 decreases. This can be seen from the increase of *sof* for the Cu_2Ag_2 substitution position (Fig. 4a), which is in a good agreement with the electric conductivity data. An increase of the maximal distance between the moving ion positions which is a limiting factor for the migration of cations in the crystal, is also observed (Fig. 6b). This fact is in a good agreement with an increase of the activation energy values for $(\text{Cu}_{1-x}\text{Ag}_x)_7\text{GeS}_5\text{I}$ solid solutions.

4. Conclusions

$(\text{Cu}_{1-x}\text{Ag}_x)_7\text{GeS}_5\text{I}$ solid solutions were obtained by a developed vertical zone crystallization method. These compounds form face-centered cubic lattice (space group $F\bar{4}3m$) with 4 formula units per a unit cell. The increase of the cubic lattice parameter in $(\text{Cu}_{1-x}\text{Ag}_x)_7\text{GeS}_5\text{I}$ solid solutions with increasing Ag content is observed. The electric conductivity of $(\text{Cu}_{1-x}\text{Ag}_x)_7\text{GeS}_5\text{I}$ crystals follows the Arrhenius law. The compositional studies have shown that the electric conductivity of $(\text{Cu}_{1-x}\text{Ag}_x)_7\text{GeS}_5\text{I}$ solid solutions decreases with silver content, but increases for the compound with $x = 1$. The highest activation energy of conductivity was obtained for $(\text{Cu}_{0.5}\text{Ag}_{0.5})_7\text{GeS}_5\text{I}$ solid solution, which is explained by the maximal distance between the mobile ion positions, which is a limiting factor for the cation migration. The structural changes in $[\text{Cu}(\text{Ag})\text{S}_3\text{I}_2]$ doubled tetrahedron show that the site occupation factor for mobile ions in $(\text{Cu}_{1-x}\text{Ag}_x)_7\text{GeS}_5\text{I}$ solid solutions with $x = 0.25, 0.5, \text{ and } 0.75$ increases compared to $\text{Cu}_7\text{GeS}_5\text{I}$ and $\text{Ag}_7\text{GeS}_5\text{I}$ compounds, which causes a decrease of the ion mobility and the electric conductivity. Hence, a good correlation between the structural and electrical properties of $(\text{Cu}_{1-x}\text{Ag}_x)_7\text{GeS}_5\text{I}$ solid solutions was observed.

Acknowledgement

This research was funded by the European Social Fund under No 09.3.3-LMT-K-712 “Development of Competences of Scientists, other

Researchers and Students through Practical Research Activities”.

References

- [1] T. Nilges, A. Pfitzner, A structural differentiation of quaternary copper argyrodites: structure – property relations of high temperature ion conductors, *Z. Kristallogr.* 220 (2005) 281–294.
- [2] S. Wenzel, S.J. Seldmaier, C. Dietrich, W.G. Zeier, J. Janek, Interfacial reactivity and interphase growth of argyrodite solid electrolytes at lithium metal electrodes, *Solid State Ionics* 318 (2018) 102–112.
- [3] A. Nagel, K.-J. Range, Verbindungsbildung im System $\text{Ag}_2\text{S}-\text{GeS}_2-\text{AgI}$, *Z. Naturforsch.* (33 b) (1978) 1461–1464.
- [4] A. Nagel, K.-J. Range, Die Kristallstruktur von $\text{Ag}_7\text{GeS}_5\text{I}$, *Z. Naturforsch.* (34 b) (1979) 360–362.
- [5] I.P. Studenyak, M. Kranjčec, Gy.Sh. Kovacs, I.D. Desnica-Frankovic, A.A. Molnar, V.V. Panko, V.Yu. Slivka, Electrical and optical absorption studies of $\text{Cu}_7\text{GeS}_5\text{I}$ fast-ion conductor, *J. Phys. Chem. Solids* 63 (2002) 267–271.
- [6] M. Laqibi, B. Cros, S. Peytavin, M. Ribes, New silver superionic conductors $\text{Ag}_7\text{XY}_5\text{Z}$ ($X = \text{Si, Ge, Sn; Y = S, Se; Z = Cl, Br, I}$) – synthesis and electrical studies, *Solid State Ionics* 23 (1987) 21–26.
- [7] I.P. Studenyak, O.P. Kokhan, M. Kranjčec, M.I. Hrehyn, V.V. Panko, Crystal growth and phase interaction studies in $\text{Cu}_7\text{GeS}_5\text{I}-\text{Cu}_7\text{SiS}_5\text{I}$ superionic system, *J. Cryst. Growth* 306 (2007) 326–329.
- [8] I.P. Studenyak, O.P. Kokhan, M. Kranjčec, V.V. Bilanchuk, V.V. Panko, Influence of S → Se substitution on chemical and physical properties of $\text{Cu}_7\text{Ge}(\text{S}_{1-x}\text{Se}_x)_5\text{I}$ superionic solid solutions, *J. Phys. Chem. Solids* 68 (2007) 1881–1884.
- [9] A. Dziaugys, J. Banys, A. Kežionis, V. Samulionis, I. Studenyak, Conductivity investigations of $\text{Cu}_7\text{GeS}_5\text{I}$ family fast-ion conductors, *Solid State Ionics* 179 (2008) 168–171.
- [10] I.P. Studenyak, V.V. Bilanchuk, O.P. Kokhan, Yu.M. Stasyuk, A.F. Orliukas, A. Kežionis, E. Kazakevičius, T. Šalkus, Electrical conductivity, electrochemical and optical properties of $\text{Cu}_7\text{GeS}_5\text{I}-\text{Cu}_7\text{GeSe}_5\text{I}$ superionic solid solutions, *Lith. J. Phys.* 49 (2009) 203–208.
- [11] I.P. Studenyak, M. Kranjčec, V.V. Bilanchuk, O.P. Kokhan, A.F. Orliukas, A. Kežionis, E. Kazakevičius, T. Šalkus, Temperature and compositional behaviour of electrical conductivity and optical absorption edge in $\text{Cu}_7\text{Ge}(\text{S}_{1-x}\text{Se}_x)_5\text{I}$ mixed superionic crystals, *Solid State Ionics* 181 (2010) 1596–1600.
- [12] I.P. Studenyak, M. Kranjčec, V.V. Bilanchuk, A. Dziaugys, J. Banys, A.F. Orliukas, Influence of cation substitution on electrical conductivity and optical absorption edge in $\text{Cu}_7(\text{Ge}_{1-x}\text{Si}_x)_5\text{I}$ mixed crystals, *Semicond. Phys. Quantum Electron.* 15 (2012) 227–231.
- [13] H.M. Rietveld, A profile refinement method for nuclear and magnetic structures, *J. Appl. Crystallogr.* 2 (1969) 65–71.
- [14] L.B. McCusker, R.B. Von Dreele, D.E. Cox, D. Louër, P. Scardi, Rietveld refinement guidelines, *J. Appl. Crystallogr.* 32 (1999) 36–50.
- [15] A. Altomare, M.C. Burla, M. Camalli, B. Carrozzini, G. Cascarano, C. Giacovazzo, A. Guagliardi, A.G.G. Moliterni, G. Polidori, R. Rizzi, EXPO: a program for full powder pattern decomposition and crystal structure solution, *J. Appl. Crystallogr.* 32 (1999) 339–340.
- [16] A. Altomare, C. Cuocci, C. Giacovazzo, A. Moliterni, R. Rizzi, N. Corriero, A. Falcicchio, EXPO2013: a kit of tools for phasing crystal structures from powder data, *J. Appl. Crystallogr.* 46 (2013) 1231–1235.
- [17] K. Momma, F. Izumi, VESTA 3 for three-dimensional visualization of crystal, volumetric and morphology data, *J. Appl. Crystallogr.* 44 (2011) 1272–1276.
- [18] A. Kežionis, E. Kazakevičius, T. Šalkus, A.F. Orliukas, Broadband high frequency impedance spectrometer with working temperatures up to 1200 K, *Solid State Ionics* 188 (2011) 110–113.
- [19] A. Kežionis, S. Kazlauskas, D. Petrušionis, A.F. Orliukas, Broadband method for the determination of small sample's electrical and dielectric properties at high temperatures, *IEEE Trans. Microw. Theory Tech.* 62 (2014) 2456–2461.
- [20] I.P. Studenyak, M. Kranjčec, Gy.S. Kovacs, I.D. Desnica-Franković, V.V. Panko, P.P. Guranich, Electric conductivity and optical absorption edge of $\text{Cu}_6\text{P}(\text{Se}_x\text{S}_{1-x})_5\text{I}$ fast-ion conductors in the selenium-rich region, *J. Phys. Chem. Solids* 62 (2001) 665–672.
- [21] I.P. Studenyak, M. Kranjčec, Gy.Sh. Kovacs, I.D. Desnica, V.V. Panko, V.Yu. Slivka, Influence of compositional disorder on optical absorption processes in $\text{Cu}_6\text{P}(\text{S}_{1-x}\text{Se}_x)_5\text{I}$ crystals, *J. Mater. Res.* 16 (2001) 1600–1608.